23. Sodar and RASS

Stefan Emeis

Vertical profiles of the wind speed, turbulence components, and the temperature in the lower regions of the atmospheric boundary layer can be determined by performing active acoustic and radioacoustic sounding with ground-based devices. This chapter introduces two types of instruments—sound detection and ranging (sodar) devices and radioacoustic sounding systems (RASS)—that can be used to carry out such measurements. While sodars can provide quantitative vertical wind and turbulence profiles and qualitative mixed-layer height and inversion height data, RASS can provide that as well as quantitative temperature profiles. Both types of instruments have a typical height range of several hundreds of meters, and their vertical resolution is on the order of 20 m.

Ground-based sonic/sound detection and ranging (sodar) devices and radioacoustic sounding systems (RASS) are active remote-sensing devices that are used to observe boundary-layer wind, turbulence, and—in the case of RASS—temperature profiles (see [23.1] for an overview of all ground-based remote-sensing techniques that are used to investigate and monitor the atmospheric boundary layer). A sodar evaluates the Doppler shifts of sound waves backscattered due to refraction index fluctuations caused by the small temperature and humidity gradients present in atmospheric turbulence, whereas a RASS emits electromagnetic and acoustic waves and uses one of them (either electromagnetic or acoustic waves) to follow the propagation of the other (acoustic or electromagnetic waves, respectively), which permits the determination of the speed of sound and thus the temperature of the atmosphere.

23.1 Measurement Principles and Parameters

Sodar and RASS devices are used to obtain boundary layer profiles of wind, turbulence, and temperature. Note that, just like many well-established and commonly used abbreviations (such as *radar*), *sodar* and *lidar* are often written in lowercase letters—as they are throughout this chapter. However, the acronym RASS is still generally written in uppercase letters.

23.1.1 Relevance of Wind, Turbulence, and Temperature Measurements of the Atmospheric Boundary Layer

Temperature, humidity, and wind are the main parameters that determine the vertical structure of the atmospheric boundary layer. While the vertical profiles of temperature and humidity are mainly responsible for the static stability of this layer, wind and turbulence dominate the dynamics of the boundary layer.

The static and dynamic states of the boundary layer dictate the strengths and the directions of fluxes of energy, momentum, and other atmospheric constituents (humidity and pollutants) between the Earth's surface and the atmosphere. The strengths of these fluxes correlate with shear and turbulence intensity. The direction is given by the gradient of the mean of the transported property.

The horizontal and vertical dispersions of pollutants correlate with the turbulence intensity. Pollutants that have been dispersed upward by turbulence and are transported upward by thermal convection during the day can undergo considerable horizontal displacement during the night due to stronger winds or even low-level jets [23.2] above the stable near-surface layer.

Wind turbines have become much larger in recent years. Hub heights of between 100 and 150 m are common for modern onshore turbines [23.3]. These turbines operate in the Ekman layer. Remote sensing is the only meaningful way to detect and monitor winds and turbulence at these heights (see Chap. 51 for further details).

23.1.2 Measured Parameters

In contrast to other meteorological variables, the wind is a vector, i.e., it is characterized by a magnitude (the wind speed) and a direction (the wind direction). Generally (except in small-scale and convective processes), the vertical wind component is much smaller than the horizontal wind components, so often only horizontal wind speeds are measured. Furthermore, wind is a highly variable atmospheric parameter; its speed and direction fluctuate strongly. This phenomenon is called the gustiness of the wind.

In the following, x and y are the two horizontal directions (positive towards the east and the north, respectively), z is the vertical direction (positive upward), and $u(t)$, $v(t)$, and $w(t)$ are the three instantaneous time-dependent wind components in the three directions x, y, and z. The following wind speeds can be defined (see Tables 23.1 and 23.2):

- The mean wind speed

$$\overline{u} = \frac{1}{T}\int_0^T \sqrt{u^2(t) + v^2(t) + w^2(t)}\,\mathrm{d}t\,, \qquad (23.1)$$

- The mean horizontal wind speed

$$\overline{u}_\mathrm{h} = \frac{1}{T}\int_0^T \sqrt{u^2(t) + v^2(t)}\,\mathrm{d}t\,, \qquad (23.2)$$

- And the mean vertical velocity

$$\overline{w} = \frac{1}{T}\int_0^T w(t)\,\mathrm{d}t\,, \qquad (23.3)$$

where the integral in the following equations is always taken from time $t = 0$ to the end of the time period T over which the speeds are averaged.

Furthermore, sodars and RASS are able to observe the variance of the vertical wind component (see Tables 23.1 and 23.2)

$$\sigma_\mathrm{w} = \sqrt{\frac{1}{T}\int_0^T (\overline{w} - w(t))^2\,\mathrm{d}t}\,. \qquad (23.4)$$

The only turbulence parameter obtained using sodar and RASS is the variance of the vertical velocity component σ_w.

The acoustic temperature T_s (Table 23.2) can be obtained using a RASS. The exact definition of this temperature, which is very similar to the virtual temperature, is given in (23.10) in Sect. 23.3.1 below.

23.1.3 Siting Considerations

Sodars and RASS are sensitive to noise but they also produce noise. This is also true of electromagnetic radiation for RASS. This limits the selection of possible sodar or RASS measurement sites and implies that sodars and RASS cannot be operated close together

Table 23.1 Parameters derived from sodar measurements

Parameter	Description	Unit	Symbol
Radial wind components	Doppler analysis only permits the derivation of radial velocities; sodar detects radial velocities sequentially in at least three different directions using the Doppler beam swinging (DBS) technique	$\mathrm{m\,s^{-1}}$	$u_1, u_2, \ldots, u_n$
Cartesian wind components	Computed from the radial wind components using trigonometric relations	$\mathrm{m\,s^{-1}}$	u, v, w
Radial turbulence component	Only the vertical component of the turbulence can be determined using vertical sounding; it is derived from either the broadening of the frequency of the backscattered signal or the temporal fluctuations in the vertical velocity component	$\mathrm{m\,s^{-1}}$	σ_w
Mixed-layer depth	Determined from the backscatter intensity (mainly the decrease in backscatter intensity with height) using an algorithm	m	MLH
Inversion height	Height of inversion is determined from the secondary maximum in the backscatter intensity	m	

Table 23.2 Parameters that are derived from RASS measurements

Parameter	Description	Unit	Symbol
Acoustic temperature	Vertical profile is determined from a vertically propagating sound pulse	K	T_s
Radial wind components (Doppler RASS only)	Doppler analysis only allows the evaluation of radial velocities; sodar detects radial velocities sequentially in at least three different directions via the Doppler beam swinging (DBS) technique	$\mathrm{m\,s^{-1}}$	$u_1, u_2, \ldots, u_n$
Cartesian wind components (Doppler RASS only)	Computed from the radial wind components using trigonometric relations	$\mathrm{m\,s^{-1}}$	u, v, w
Radial turbulence component (Doppler RASS only)	Only the vertical component of turbulence can be determined using vertical sounding; it is derived from either the broadening of the frequency of the backscattered signal or the temporal fluctuation of the vertical velocity component	$\mathrm{m\,s^{-1}}$	σ_w
Mixed-layer depth (Doppler RASS only)	Determined from the acoustic backscatter intensity (mainly the decrease in the backscatter intensity with height) using an algorithm	m	MLH

(within a few hundreds of meters of each other) because they would interfere with each other. Since these instruments sound mainly in the vertical direction, the chosen measurement site must provide a free sky view. Public access to operational instruments of this type should be prohibited for two reasons. On the one hand, vandalism must be discouraged. On the other hand, the acoustic and electromagnetic radiation emitted from the instruments can be harmful to humans. The noise pressure within the antennae of a three-antenna sodar or the enclosure of a phased-array sodar can damage ear drums. Spending an extended period at distances of up to $\approx 4\,\mathrm{m}$ from the sending electromagnetic antenna of a RASS can also be harmful.

Both types of instruments need a steady power supply, which can be provided by either the grid or a system of solar panels connected to an energy storage unit. The transportation of such heavy instrumentation to the intended site requires access roads that are suitable for use by heavy-duty vehicles (this includes sufficient vertical clearance all the way to the measurement site!). Sections 23.3.1 (on fixed echoes), 23.5.2, and 23.5.3 give additional information on the requirements for sites at which these instruments can be operated.

23.1.4 Measurement Principles of Sodars

A sodar consists of a pulsed sound emitter and a receiver [23.4]. Sound waves are scattered by turbulent temperature fluctuations in the atmosphere, since the refractive index for sound waves changes at the boundaries of these fluctuations. The fluctuations that reflect the sound pulses emitted from the sodar are assumed to move with the mean wind. Therefore, acoustic waves that are backscattered in the atmosphere are Doppler shifted in frequency if the air is in motion. Sodars that analyze the Doppler shift of the backscattered sound pulses in order to determine the vertical wind profile are called *Doppler sodars* (see Table 23.3 and Fig. 23.2 for instrument terminology). The Doppler shift is proportional to the radial velocity v_r (see Tables 23.1 and 23.2 and Sect. 23.3.2). The range is dictated by the travel time of the pulse and the backscattered wave. An overview of the basic principle of sounding with a sodar and the history of sodar development are described in [23.5]; a summary of acoustic remote-sensing techniques and their theoretical background was recently provided by *Bradley* [23.6].

Table 23.3 Measurement principles for wind, turbulence, and temperature, and applications of such measurements

Parameter	Measurement principle			Application	
	Doppler	Backscatter intensity	Sound speed	Mean	Turbulent
Wind	×			×	
Turbulence	×	×			×
Temperature gradient		×			×
Temperature			×	×	

Sodar measurements depend on the state of the atmosphere. If the atmosphere is extremely well mixed (i.e., temperature fluctuations are very small), almost no sound is reflected from the atmosphere, and the signal-to-noise ratio for sodar can be so low that it is not possible to accurately determine the wind speed (via the Doppler shift). Such a scenario tends to occur during the afternoon on days with low mean wind speeds and strong vertical mixing due to thermal heating.

For optimal backscatter, the spatial size of temperature gradients in the atmosphere should be about half the acoustic wavelength (Bragg condition) [23.7]. This condition can be fulfilled by the temperature gradients within turbulence elements as well as those across inversion layers. It is necessary to differentiate between these two possibilities when deducing information on the atmospheric state from the backscattered signal. This can be done by either assessing the general weather conditions or, if a Doppler sodar is used, by analyzing the variance of the simultaneously recorded vertical velocity. High variances indicate thermal forcing, where the backscatter intensity is proportional to the turbulence intensity, whereas low variances indicate stable layering, where the backscatter intensity should be proportional to the mean vertical temperature gradient (i.e., inversion).

For a sodar (just as for radar), the backscattered signal is representative of a certain atmospheric volume. If the duration of the sound pulse is 100 ms, the sodar detects simultaneous backscatter from a volume 33 m deep. If this volume is 500 m AGL, it has a radius of 44 m (assuming that the opening angle of a single emitted sound beam is 5°). Additionally, the three-dimensional wind information must be integrated from a full measurement cycle comprising one vertical and two to four tilted beams (see the description of the Doppler beam swinging technique in Sect. 23.4.1). This implies that the radius of the detected atmospheric volume at a height of 500 m AGL is about 150–200 m. This means that a sodar performs volume- and time-averaged measurements.

23.1.5 Measurement Principles of RASS

A radioacoustic sounding system (RASS) performs acoustic and electromagnetic sounding simultaneously [23.8, 9]. Two different types of RASS have been developed: the Bragg RASS and the Doppler RASS [23.10].

The *Bragg RASS* (sometimes called a wind-temperature radar) is a wind profiler (see Chap. 31 and [23.11]) with an additional acoustic emitter. When the Bragg condition is fulfilled [23.7] (i.e., the wavelength of the sound waves λ_a is half the wavelength of the electromagnetic waves λ_e, see Tables 23.4 and 23.5), there is optimal backscatter of the electromagnetic waves from the acoustic waves. The electromagnetic signal is emitted at a fixed frequency, but the emitted sound has a continuously varying frequency f_a. The propagation speed of the acoustic signal can be determined from the acoustic wavelength $\lambda_{a,B}$ at which optimal backscatter occurs via the dispersion relation

$$c = \frac{\lambda_{a,B}}{2} f_a \,. \tag{23.5}$$

A sound frequency of about 100 Hz is used for a VHF wind profiler operating at 50 MHz, while a sound frequency of ≈ 2 kHz optimally fulfills the Bragg condition for an UHF wind profiler operating at 1 GHz. Because the attenuation of sound waves in the atmosphere depends strongly on frequency [23.12], an UHF RASS can detect the temperature profile up to a height of ≈ 1.5 km, whereas a VHF RASS can determine the temperature profile throughout the troposphere.

Table 23.4 Parameters that are measured using sodar

Parameter	Description	Unit	Symbol
Frequency	The mean frequency and the width of the frequency spectrum of the backscattered signal are recorded as functions of propagation time	s^{-1}	f_a
Acoustic backscatter intensity	Parameter is recorded as a function of propagation time	dB	P_R

Table 23.5 Parameters that are measured using a RASS

Parameter	Description	Unit	Symbol
Acoustic frequency (Doppler RASS only)	Mean frequency and width of the frequency spectrum of the backscattered signal are recorded as functions of the propagation time	s^{-1}	f_a
Acoustic backscatter intensity	Parameter is recorded as a function of propagation time	dB	P_R
Electromagnetic frequency	Mean frequency and width of the frequency spectrum of the backscattered signal are recorded as functions of the propagation time	s^{-1}	f_e

Table 23.6 Additional parameters that are required to interpret sodar measurements

Parameter	Description	Unit	Symbol
Atmospheric temperature	Needed to determine the speed of sound, which is then used to derive the distance from the scattering volume	K	T
Orientation, alignment	Orientation with respect to north is needed to convert radial wind velocities into Cartesian wind components; instrument should be aligned horizontally	degrees	
Distance to scattering objects	The distance to possible scattering objects (trees, buildings, electricity cables, ...) must be known in order to identify fixed echoes	m	

A *Doppler RASS* is a sodar with an additional electromagnetic emitter and receiver operating at a frequency of $f_{e,0}$. This instrument is able to detect the acoustic shock fronts of the acoustic pulses and determine their propagation speed from the backscattered electromagnetic waves. This propagation speed is equal to the speed of sound, which is in turn a known function of the air temperature (see also Tables 23.6) and humidity. Using the Doppler shift Δf_e (see Sect. 23.3.3) of the electromagnetic radiation backscattered at the density fluctuations caused by the sound waves, the propagation speed c of the sound waves can be determined as

$$c = 0.5 c_l \frac{\Delta f_e}{f_{e,0}} , \tag{23.6}$$

where c_l denotes the speed of light. Just like a Bragg RASS, a Doppler RASS emits a *chirp* (a sound signal) to check that the Bragg condition is optimally met, considering that the temperature varies significantly across the entire height interval considered.

The propagation speed c_g is the sum of the speed of sound c and the vertical movement of the air w in which the sound waves propagate, i.e.,

$$c_g = c + w . \tag{23.7}$$

The vertical air speed component w can be determined separately from the Doppler shift of the backscattered electromagnetic clear-air signal when operating a Bragg RASS, or from the Doppler shift of the backscattered acoustic signal when operating a Doppler RASS. The height profile of c can then be converted into a height profile for the acoustic temperature T_s (see Sect. 23.3.1). This acoustic temperature is a sufficiently accurate approximation of the virtual air temperature for many applications.

A Bragg RASS has a greater maximum range than a Doppler RASS but a coarser height resolution. A Doppler RASS is also much easier to implement than a Bragg RASS, meaning that a Doppler RASS is less expensive.

23.2 History

The development of ground-based remote-sensing devices started during World War II with the construction of the first weather radars [23.13]. The first acoustic wind profilers (sodars) were invented shortly after World War II. The idea for a RASS device originated in the early 1970s.

23.2.1 History of Sodar Measurements

Acoustic sounding technology was developed shortly after World War II [23.14]. Most of the theoretical foundations for this field were laid by *Valerian Iljitsch Tatarskij* [23.15], with the initial development of acoustic sounding technology occurring in the Soviet Union [23.16, 17] and (a decade later) in the United States [23.18]. Analyzing the backscatter intensity was the main focus in the beginning. More recently, the emergence of wind energy applications in the last decade of the twentieth century has fostered renewed interest in this wind measurement technology. The use of Doppler analysis to derive wind speed is now the main application of acoustic sounding technology. However, the rapid development of optical Doppler wind lidars between 2005 and 2010 heavily suppressed

further development in the field of sodar devices. Although optical techniques are much more expensive than acoustic techniques, optical techniques have become more popular because they do not suffer as much from environmental interference and because they have higher data availability during a given time period (see Chap. 27 for further discussion of Doppler wind lidars).

23.2.2 History of RASS Measurements

The acoustic backscatter intensity gives only a very crude estimate of the vertical temperature gradient. This led to the development of the RASS nearly 50 years ago [23.8]. RASS were constructed by either adding a radar component to a sodar (Doppler RASS) or by adding a sound component to a wind profiler (Bragg RASS). Although RASS suffer from the same environmental interference as sodar devices, they have not been superseded by optical techniques so far. Passive radiometers (Chap. 29) have come onto the market, but they do not offer the same high vertical resolution as RASS. Raman lidars (Chap. 25) are much more expensive and have poor signal-to-noise ratios during the daytime due to interference from scattered sunlight.

23.3 Theory

The following sections provide the theoretical background for both sodars and RASS. The theory behind the propagation of acoustic waves in the atmosphere is utilized for both types of instruments, while the theory behind the propagation of radio waves is only employed for RASS.

23.3.1 Sound Propagation in the Atmosphere

Sound waves are elastic vibrations that propagate as longitudinal waves (i.e., the material vibrates in the same direction as the direction of propagation of the sound wave). For ideal gases, the speed of sound c is given by

$$c = (\gamma RT)^{0.5} , \tag{23.8}$$

where γ is the ratio of the specific heats (c_p/c_v), R is the specific gas constant of an ideal gas in $\mathrm{J\,kg^{-1}\,K^{-1}}$, and T is the absolute temperature in K.

The speed of sound in air is mainly a function of the temperature. Nevertheless, changes in the humidity of the air affect both R and γ, so the speed of sound also depends on the humidity. If the humidity is given in terms of the partial pressure e or the specific humidity q, the speed of sound in humid air can be expressed as

$$c = (\gamma_{tr} R_{tr} T_s)^{0.5} = 20.048 (T_s)^{0.5} , \tag{23.9}$$

where γ_{tr} is the ratio of the specific heats for dry air, R_{tr} is the gas constant of dry air in $\mathrm{J\,kg^{-1}\,K^{-1}}$, and T_s is the acoustic temperature in K, as given by

$$T_s \approx T\left(1 + 0.329\frac{e}{p}\right) \approx T(1 + 0.531q) , \tag{23.10}$$

where p is the air pressure in the same units as e.

T_s is very similar to the virtual temperature T_v that is commonly used for humid air in meteorology, although it differs from it slightly, as described by

$$T_s = T_v - 0.0489\frac{eT}{p} \tag{23.11a}$$

or

$$T_s = T_v - 0.079q , \tag{23.11b}$$

where T, T_s, and T_v are in K, e and p are in hPa, and q is in $\mathrm{kg\,kg^{-1}}$.

Attenuation of Sound Waves in the Atmosphere

The attenuation of sound waves in the atmosphere depends on the frequency, temperature, and humidity. The attenuation-dependent transmittance follows the Bouguer–Lambert–Beer law

$$\tau(x,f) = \exp\left(-\int_0^x \alpha(x',f)\mathrm{d}x'\right) , \tag{23.12}$$

where the absorption coefficient $\alpha(x,f)$ is in $\mathrm{m^{-1}}$ and

$$\alpha = f^2\left[1.84\times10^{-11}\frac{p_r}{p}\left(\frac{T}{T_{20}}\right)^{1/2} + \left(\frac{T}{T_{20}}\right)^{5/2} \times\left(\frac{f_{O_2}\times0.01275\times\exp(-2239.1/T)}{f_{O_2}^2+f^2} + \frac{f_{N_2}\times0.1068\times\exp(-3352/T)}{f_{N_2}^2+f^2}\right)\right] , \tag{23.13}$$

where p_r is a constant pressure (1013.25 hPa), p is the surface pressure at the observation site in hPa, T is the

absolute surface temperature in K, and T_{20} is a constant temperature (293.15 K).

Equation (23.13) requires two relaxation frequencies: f_{O2} for oxygen, as given by

$$f_{O_2} = \frac{p}{p_r}\left[24 + 4.04\times10^4 h\left(\frac{0.02+h}{0.391+h}\right)\right], \tag{23.14a}$$

and f_{N_2} for nitrogen, evaluated using

$$f_{N_2} = \frac{p}{p_r}\left(\frac{T}{T_{20}}\right)^{1/2}\left[9 + 280h \times \exp\left(-4.170\left(\left(\frac{T}{T_{20}}\right)^{-1/3} - 1\right)\right)\right]. \tag{23.14b}$$

Both of these relaxation frequencies also depend on the relative humidity

$$h = 100\frac{e}{p}, \tag{23.14c}$$

where h is in %. Further details can be found in [23.12, 19, 20].

Apart from shock waves (described in Sect. 23.3.3), the propagation of electromagnetic waves is only marginally influenced by atmospheric properties, so they can be neglected here.

Backscattering of Sound Pulses in the Atmosphere

Turbulent inhomogeneities of the temperature, humidity, and wind velocity lead to local changes in the speed of sound and thus to the scattering of some of the sound energy. This process is referred to as clear air scattering or Bragg scattering. In backscattering (scattering angle $= 180°$), only temperature and humidity inhomogeneities (not wind velocity fluctuations) contribute to the scattered signal. Backscattering is most effective when it occurs at turbulent structures with sizes that are half the wavelength of the sound wave (the Bragg condition). Scattering also occurs at precipitation particles.

When an emitting power of $\approx 1\,\mathrm{kW}$ is used, a backscattered signal with a power of $\approx 10^{-15}\,\mathrm{W}$ is obtained. This is below the hearing threshold of the human ear ($10^{-12}\,\mathrm{W}$) but well above the noise produced by the Brownian motion of atmospheric molecules ($6\times10^{-19}\,\mathrm{W}$). The sound frequencies used (1500–4500 Hz) are well within the sensitivity range of the human ear.

The ratio of the emitted to the received power is given by the sodar equation

$$P_R = r^{-2}\left(\frac{c\tau_d A\varepsilon}{2}\right)P_0\beta_s\exp(-2\alpha r) + P_{bg}, \tag{23.15}$$

where P_R is the received power, P_0 is the emitted power, r is the distance between the sodar and the scattering element, ε is the antenna efficiency, A is the effective antenna area, τ_d is the pulse duration (typically between 20 and 100 ms), β_s is the backscattering cross-section (typically on the order of $10^{-11}\,\mathrm{m^{-1}\,sr^{-1}}$), and P_{bg} is the background noise.

The speed of sound c and the absorption coefficient α are defined in (23.8) and (23.13) above. The background noise also includes contributions from ambient noise with the same sound frequency, e.g., traffic noise. The ratio of the two terms on the right-hand side of the sodar equation is called the signal-to-noise ratio (usually abbreviated to SNR). The backscattering cross-section β_s is a function of the temperature structure function C_T^2 [23.15]. When using the wavenumber $k = 2\pi/\lambda$ for a monostatic sodar, we find that

$$\beta_s(180°) = 0.00408k^{1/3}\frac{C_T^2}{T^2}. \tag{23.16}$$

This equation gives an average over all scattering elements within the atmospheric volume that is hit by the cone-shaped beam [23.21].

Fixed Echoes

Sodar beams also have side lobes. If these side lobes hit highly reflective obstacles, sound energy with a strength that is similar to or even much stronger than the atmospheric return is scattered back towards the instrument. The backscattered signals from these objects are called fixed echoes. Fixed echoes can strongly influence and disturb sodar measurements. Since fixed echoes are reflected from fixed (i.e., stationary) objects, they cause the deduced wind speed to be much lower than it really is. Avoiding fixed echoes requires good measurement site selection for sodar instruments in order to guarantee unbiased wind speed measurements. Sodars must therefore be sited away from obstacles such as buildings, trees, and—most importantly—electric transmission cables. If the sodar has to be sited near such objects, it should be situated such that the distance to the highly reflecting objects does not conflict with the range of the atmospheric layers that are to be investigated. This often means positioning the sodar closer to such objects than the lowest range gate of the instrument (usually $\approx 40\,\mathrm{m}$).

23.3.2 Doppler Analysis

Wind and turbulence are measured with a sodar by analyzing the Doppler shift of the backscattered acoustic pulse that was originally emitted with a frequency f_0. Assuming that the scattering volume for the sound waves is moving with the wind, the Doppler-shifted sound frequency f_D is given by

$$f_D = f_0 \frac{c - v_r}{c + v_r} , \tag{23.17}$$

where v_r is the radial velocity along the path of the emitted sound beam (positive away from the sodar) and f_0 the emitted acoustic frequency. Solving for the radial velocity v_r gives

$$v_r = c \frac{f_0 - f_D}{f_0 + f_D} . \tag{23.18}$$

23.3.3 Principle of Radioacoustic Sounding

Measurements are achieved using a RASS by modifying the propagation conditions for electromagnetic waves in a controlled manner using sound waves. The scattering of electromagnetic waves from refractive-index modifications generated by acoustic waves differs from scattering due to atmospheric turbulence (such as that used for wind profiler radar measurements) in several respects [23.9]:

1. Modifications of the atmospheric refractive index propagate as spherical waves at the speed of sound, whereas moving refractive-index variations caused by natural turbulence do not show any systematic behavior.
2. The spherical wavefronts focus the scattered electromagnetic waves. Therefore, to obtain a sufficiently high receiver signal, the antenna needs to be located near the focus (*acoustic spot*) formed by the sound waves.
3. Horizontal wind carries sound waves away and causes the focus of the backscatter signal to drift, limiting the maximum range. In a turbulent atmosphere, sound-wave scattering extends the focal area beyond that of the electromagnetic transmitter antenna, reducing the adverse effect of drift on the maximum range.
4. Atmospheric absorption also decreases the sound intensity, leading to a reduction in the maximum range of the RASS, similar to that for a sodar.
5. The backscatter signal is maximized when the ratio of the electromagnetic to the acoustic wavelengths is $2:1$ ($\lambda_e = 2\lambda_a$, known as the Bragg condition; see Fig. 23.1).

When the Bragg condition is met, the power $P_s(z)$ received at the RASS is described by the RASS equation

$$P_s(z) = 0.588 \times 10^{-14} c_g \frac{\Delta z}{(\lambda_e z)^2} \frac{P_a P_e}{B_a} g \tau I P_{N,N_0} , \tag{23.19}$$

where P_{N,N_0} is the normalized backscatter power for $N = N_0$, N is the number of acoustic waves within the scattering volume Δz (the backscatter power is proportional to N^2), P_a is the transmitted acoustic power, P_e is the transmitted electromagnetic power, B_a is the acoustic bandwidth, g is a gain parameter ($g = g_a$ if $g_e \geq g_a$; otherwise, $g = g_e^2/g_a$), g_a is the gain of the acoustic antenna, g_e is the gain of the electromagnetic antenna, τ is the acoustic transmission due to atmospheric absorption, I is an inhomogeneity parameter that accounts for atmospheric turbulence ($I < 1$ describes a turbulent, agitated, layered atmosphere whereas $I = 1$ is indicative of a stationary, quiet, homogeneous atmosphere), and Δz is the radial extent of the scattering volume.

The equation used to determination c_g depends on the type of RASS employed. For a Doppler RASS, we have

$$c_g = -\frac{\lambda_e}{2} \Delta f_e \approx -\lambda_a \Delta f_e . \tag{23.20}$$

For a Bragg RASS, we have

$$c_g = -\lambda_a f_B . \tag{23.21a}$$

As both Δf_e and f_B are actually equal to the acoustic frequency f_a, we find that

$$c_g = -\lambda_a f_a \tag{23.21b}$$

for both types of RASS.

Finally, the speed of sound and the radial wind component due to atmospheric motion must be separated (see (23.7)). If the effect of a nonzero radial velocity v_r is neglected when deriving the temperature T from the sound velocity c_g, the resulting error is 1.7 K per m s^{-1} of the unknown radial wind v_r. The simplest method of suppressing the effect of the vertical wind consists of pointing the RASS vertically and averaging the speed of sound c_g over a long period of time, as the long-term vertical wind over horizontal terrain tends to zero. This method is usually applied in routine measurements. In a convective atmosphere, however, usual averaging times of between 10 and 30 min may not be sufficient, resulting in a considerable error in the temperature measurement due to the vertical wind. If the terrain is tilted, the average vertical wind may be nonzero, so averaging over long periods of time is not a solution. In these

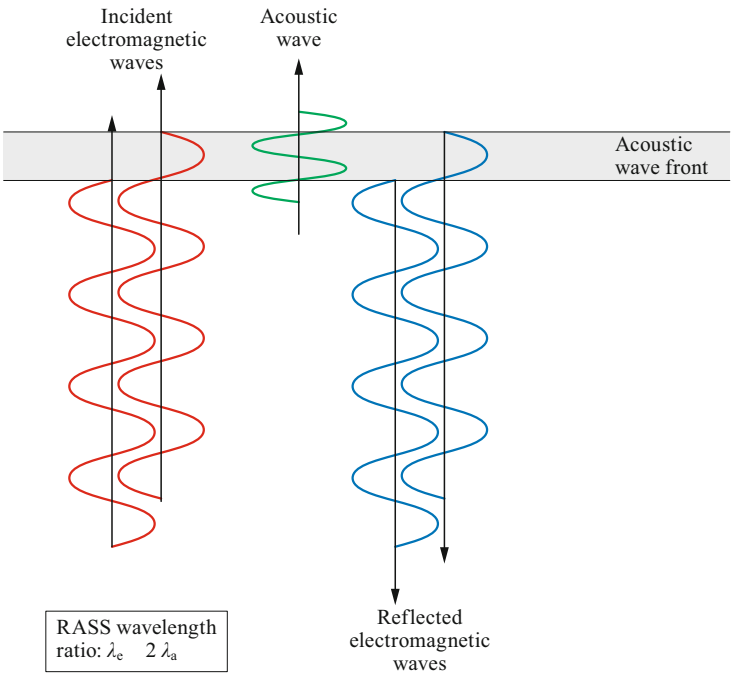

Fig. 23.1 Illustration of the Bragg condition for Doppler RASS instruments. Here, acoustic waves are shown in *green*, whereas emitted and reflected electromagnetic waves are shown in *red* and *blue*, respectively. The electromagnetic waves are reflected at the leading and trailing edges of the sound pulse. For all of the reflected electromagnetic waves to be in phase, the wavelength of the emitted electromagnetic waves must be twice the wavelength of the moving sound pulse

cases, the vertical wind component measured with the sodar (when using a Doppler RASS) or with the wind profile radar (when using a Bragg RASS) can be used for correction. The vertical temperature profile is assessed with a RASS by determining the thermodynamic speed of sound c in each altitude interval.

23.3.4 Vertical Range

The vertical range of the wind and temperature data obtained from a sodar and a Doppler RASS is determined from the travel time of the sound pulses. For a Bragg RASS, the vertical range is determined from the travel time of the electromagnetic waves. The maximum vertical range is influenced by the attenuation of sound waves in the atmosphere (see Sect. 23.3.1).

23.3.5 Vertical and Temporal Resolution

The pulse duration τ_d determines the height resolution of the instrument via the relation

$$\Delta z = 0.5 c \tau_d \, . \qquad (23.22)$$

The sodar equation (23.15) shows that the backscatter power is also proportional to the pulse duration. Therefore, the choice of pulse duration is made from a trade-off between height resolution (preferably short pulse durations) and maximum range (preferably long durations). Equation (23.19) is valid for a perfect rectangular pulse but can also be used as a good first approximation for real pulses.

To avoid unwanted interference, a new pulse cannot be emitted before the backscatter from the previously emitted beam has been received, so a measurement cycle of a sodar lasts six to ten times as long as the time needed for a sound pulse to travel to the maximum vertical range of the instrument. For a sodar or Doppler RASS operating at 1500 Hz, this implies that the duration of a measurement cycle is ≈ 20 s when the range is 1000 m.

23.3.6 Determination of the Mixed-Layer Height and Inversions

The layering of the atmospheric boundary layer due to the vertical temperature and moisture distribution and the existence of inversions within this layer or on top of it strongly influence the development of atmospheric motions and high pollutant concentrations in the air. Well-mixed layers of the atmospheric boundary layer are characterized by enhanced turbulence compared to the stably stratified free troposphere above. For a convective boundary layer (CBL), the mixed-layer height (MLH) is usually identical to the temperature inversion height.

Beyrich [23.22] has listed possible analyses of the MLH and inversions based mainly on acous-

tic backscatter intensities measured by a sodar. Asimakopoulos et al. [23.23] analyzed these methods further and grouped them into three approaches to deriving the MLH from sodar data: the horizontal wind speed (HWS) method, the acoustic received echo (ARE) method, and the vertical wind variance (VWV) method.

The ARE method is the simplest method of determining the MLH from acoustic remote sensing. Most of the methods listed in [23.22] are variants of this type. This method does not require an analysis of the Doppler shift of the backscattered signals. The MLH is derived from either the most negative slope, the change in curvature of the vertical profile of the acoustic backscatter intensity, or the height at which the backscatter intensity decreases below a certain prespecified threshold value. Inversions are found by searching for secondary maxima in the vertical profile of the backscatter intensity.

The ARE method can be enhanced in two ways. The first way is to include further variables for which data are provided by Doppler sodars in the MLH algorithm. For instance, the utilization of the variance of the vertical velocity component is demonstrated in [23.24]. The second way to enhance the ARE method is to determine not only the MLH from sodar measurements but also the heights of lifted inversions. Especially above orographically complex terrain, the vertical structure of the atmospheric boundary layer (ABL) can be very complicated [23.25]. Enhanced ARE methods (and optical methods that use ceilometers and wind lidars) are described in more detail in [23.26].

The HWS method requires an analysis of the Doppler shift of the backscattered signals. It involves analyzing the shape of hourly-averaged vertical wind-speed profiles under the assumption that wind speed and wind direction are almost constant within the mixing layer but the wind speed increases gradually towards the geostrophic value at the top of the mixing layer. Given the underlying assumptions, the applicability of this method is probably limited to well-developed CBLs. Such CBLs are often higher than the maximum range of a sodar. Even if the CBL height is within the range of the sodar, the algorithm used to analyze the Doppler shift often fails above the inversion atop the CBL due to poor signal-to-noise ratios. Therefore, this method is not recommended.

The VWV method also only works for CBLs. It focuses on the vertical profile of the variance of the vertical velocity profile σ_w. In a CBL, σ_w is usually greatest at a height that is between 0.35 and 0.4 times the inversion height. Thus, in principle, this is an extrapolation method. It has been attempted for sodar measurements because it permits MLH detection up to heights that are 2.5 times above the highest that can be probed (usually between 500 and 1000 m) with a sodar. *Beyrich* [23.22] classified this method as unreliable.

23.4 Devices and Systems

This section describes typical configurations of current sodar and RASS systems (see Fig. 23.2 for an overview of different techniques and instruments).

23.4.1 Sodars and Minisodars

The Doppler beam swinging (DBS) technique [23.27] is the standard technique used by sodars. It is different from the usual technique employed by Doppler wind lidars (see Chap. 27), which uses conical scanning to get wind information from different directions. With DBS, at least three—but often five—beams are subsequently emitted in different directions. Two (or four) beams at right angles to each other are emitted at zenith angles of $\approx 15^\circ$; the third (or fifth) beam is emitted vertically. The angle between the slanted beams should be as low as possible to receive the three (or five) different sets of information, which are later used to compute the three orthogonal wind components from air volumes that are close together. If the angle becomes too small, the computation of horizontal wind components from near-vertical radial velocity components along the beams becomes too uncertain. There is a trade-off between getting information from air volumes that are close together and the certainty with which the horizontal wind components can be computed.

The radial wind component along a beam with a zenith angle δ and an azimuth angle ϕ is composed of all three Cartesian wind components u (towards the east), v (towards north), and w (upwards), i.e.,

$$v_r(\delta, \phi) = u \sin\delta \sin\phi + v \sin\delta \cos\phi + w \cos\delta . \quad (23.23)$$

Inversely, all three Cartesian components can be computed from (at least) three radial velocities in different noncoplanar directions.

Equations (23.12) and (23.13) show that sound attenuation in the atmosphere is strongly frequency dependent. Higher frequencies are attenuated much faster than lower frequencies. Therefore, sodars that are designed to have larger ranges operate at

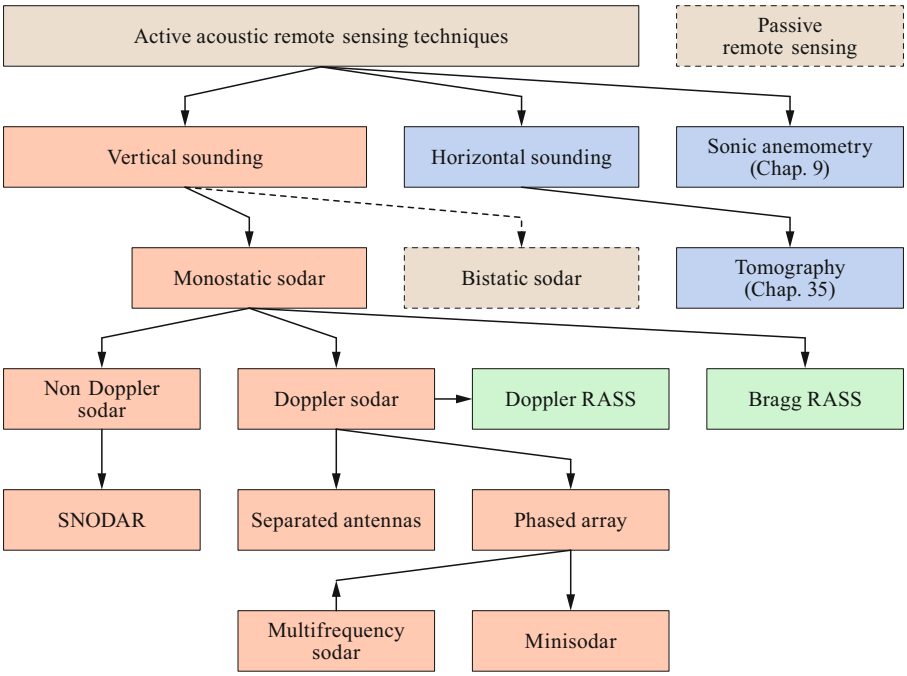

Fig. 23.2 Organigram of acoustic sounding techniques. Techniques in *brown boxes* and *green boxes* are presented in this section. Techniques in *blue boxes* are introduced in other sections. Techniques in *dashed boxes* are not relevant to this chapter

≈ 1500 Hz. However, a second class of sodars has been developed—*minisodars* [23.28]—that are optimized for short-range measurements (up to ≈ 200 m AGL). This shorter range permits more measurement cycles because the time that the sodar must wait to receive the reflected pulse is also shorter. Furthermore, environmental noise is reduced somewhat compared to standard sodars. Minisodars are usually designed for use as phased-array sodars (see Sect. 23.4.1).

Sodars with Antennas

The first Doppler sodars utilized three parabolically shaped antennas (horns) that could be aligned in three different directions (Fig. 23.3). In such systems, the bottom of each antenna has one or a few sound transducers that are operated simultaneously. The transducers first act as loudspeakers and are then switched electronically to act as microphones. The shape of the antenna helps to focus the sound beam. In addition, the antennas at least partially prevent noise interference from reaching the sound transducers and shield the region close to the instrument from excessive sound pulses, which could damage unprotected ear drums. The most suitable and common alignment used in these systems is one where two antennas are inclined by a zenith angle of ≈ 15° and have an azimuth angle of 90° between them, while the third antenna is adjusted to be precisely vertical. The sound transducers in the three antennas are operated sequentially in order to prevent interference from the other antennas. The waiting time between two sound emissions from different antennas must at least be twice the travel time of the sound pulse to the maximum range of the instrument.

Fig. 23.3 Sodar with three antennas (horns) (photo © Stefan Emeis)

Phased-Array Sodars

Phased-array sodars were first constructed in 1989 [23.29]. They are systems in which a field (array) of acoustic transducers is responsible for forming and directing beams (Fig. 23.4). Between 16 and 64 acoustic transducers are usually arranged in a planar array and adjusted to create a defined phase relationship between them. The array of transducers is operated such that sound beams are formed due to interference

Fig. 23.4 Phased-array sodar with 64 sound transducers and no enclosure (photo © Helmut Mayer)

between the sound waves from the individual loudspeakers (Fig. 23.5). These beams are comparable to the beams described above for the systems with antennas. The whole system requires an enclosure that protects the system from environmental noise and ensures that operators and people passing by do not experience dangerous sound levels.

Monostatic and Bistatic Sodars

In a monostatic sodar, the receiver is close to the emitter. The intensity of the backscattered signal depends only on temperature fluctuations in the atmospheric boundary layer. Monostatic sodars have the advantage of compactness, and the instruments are more readily deployed in the field because the instrument package is self-contained. This is the standard configuration of presently available sodars.

In a bistatic sodar, the receiver is deployed away from the emitter. In this case, velocity fluctuations in the atmosphere also contribute to the intensity of the backscattered signal. The Doppler shift and scattering cross-section for bistatic sodars were analyzed by *Thomson and Coulter* [23.30] and *Wesely* [23.31]. Early experiments with bistatic sodars are described in [23.32, 33]. While bistatic sodars have been constructed and used in experiments, there are no commercially available bistatic sodars. Recent studies utilizing these sodars can be found in [23.34, 35].

Other sodar designs [23.36] in which several receivers are arranged around one central sound source (multistatic sodars) have also been proposed. This should allow all three components of the wind to be detected for the same atmospheric volume. Such instruments could be operated in complex terrain without the need to correct for curved streamlines (see Sect. 23.6.3).

Mono- and Multifrequency Sodars

In addition to monofrequency sodars, multifrequency sodars are available. These emit a series of pulses with different frequencies within one shot. Field tests have proven that the multifrequency technique has significant advantages. The use of, say, eight different frequencies halves the minimum acceptable signal-to-noise ratio compared to single-frequency sounding. Moreover, the multifrequency mode improves the accuracy of the instantaneous values of measured parameters and significantly increases the ability to reliably recognize noisy echo signals. Further details regarding multifrequency sodars are given in [23.37].

The principles of pulse code methods that are used to enhance the range and data availability are reviewed and investigated in [23.38]. In particular, detailed simulations are performed using weather-like targets, a comb of frequencies, a chirp, and a phase-encoding method. Three Doppler-adaptive matched filters are described, and two of these are evaluated against the simulated noisy atmosphere. It is found that the comb of frequencies produces the least variance in the estimated Doppler wind speed. A filter based on a single evaluation of a Fast Fourier Transform of the received signal provides Doppler wind measurements to an accuracy of about 1%. The Doppler-adaptive filters add little computational or hardware overhead, and produce a simple output consisting of the best estimate for the wind speed component.

Non-Doppler Sodars

The first sodars were non-Doppler sodars. Later, Doppler sodars became the standard, and now nearly all commercially available sodars are Doppler sodars. Nevertheless, a few non-Doppler sodars do exist. An example is a special sodar developed for use in extremely cold environments. This SNODAR (surface layer non-

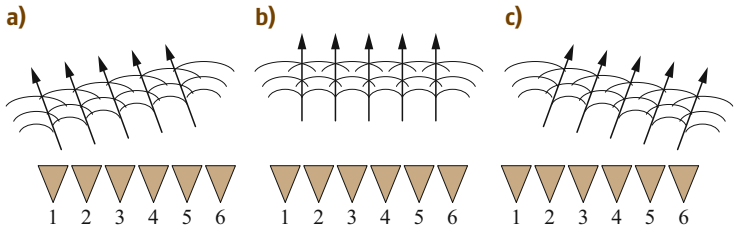

Fig. 23.5a–c Measurement principle of phased-array sodars. **(a)** Loudspeaker 6 fires first and loudspeaker 1 last, **(c)** loudspeaker 1 fires first and loudspeaker 6 last, and **(b)** all loudspeakers operate simultaneously

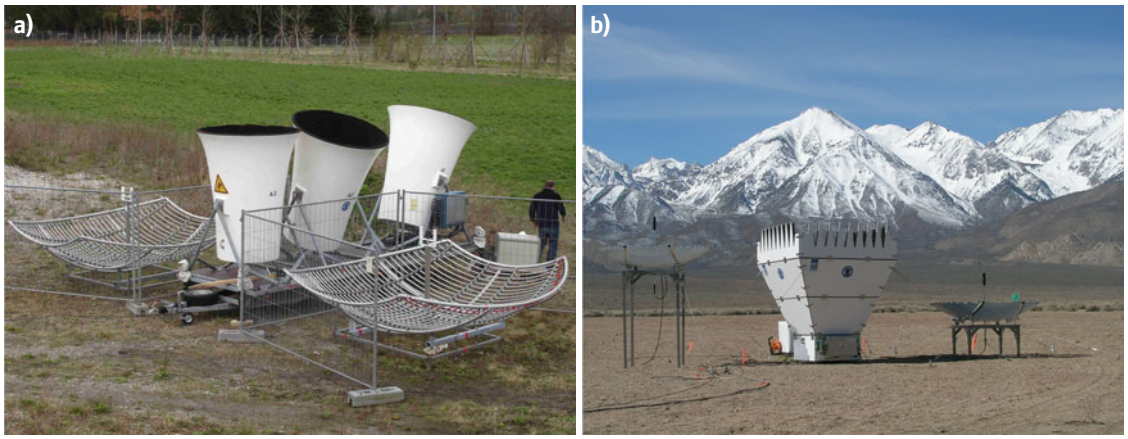

Fig. 23.6a,b Doppler RASS with the acoustic (sodar) instrument at the center and radio antennas to the left and right: **(a)** 475 MHz system (photo © Stefan Emeis); **(b)** 1290 MHz system (photo © METEK GmbH, Elmshorn)

Doppler acoustic radar) is designed to measure the height and turbulence intensity of the atmospheric boundary layer above the Antarctic plateau. This is, for example, useful to astronomers who are planning to install future optical telescopes there. SNODAR works by sending an intense acoustic pulse into the atmosphere and listening for backscatter from inhomogeneities resulting from temperature gradients and wind shear. Its operating principle is very similar to that of a well-known underwater sounding technique: SONAR. SNODARs are monostatic sodars with a minimum sampling height of 5 m, a range of at least 200 m, and a vertical resolution of 1 m. They operate at frequencies of between 4 and 15 kHz. Sound waves with such high frequencies propagate relatively well in the low temperatures of the Antarctic atmosphere [23.39].

23.4.2 RASS

There are two types of RASS. One (known as a *Doppler RASS*) is a combination of a sodar with a continuous-wave electromagnetic transmitter and receiver; the other (known as a *Bragg RASS*) is a wind profiler radar (see Chap. 31 and [23.11]) combined with a continuous sound transmitter. The latter combination is sometimes also called a wind-temperature radar (WTR).

Sodar RASS (Doppler RASS)

In today's terminology, the first RASS, which was first designed and built by *Marshall et al.* [23.8], was a Doppler RASS in which acoustic pulses were pursued by continuous electromagnetic radiation emitted from a transmitter (Fig. 23.6). Altitude assignment is achieved for a RASS by measuring the propagation time of the acoustic pulses, much as in a sodar; the time taken for the electromagnetic pulses to return is negligible. The observed frequency shift of the electromagnetic backscatter signal is interpreted as a Doppler shift. The emitted acoustic pulse is a chirp over a selected sound frequency range that is centered on the Bragg resonance frequency to guarantee that the Bragg condition is met for all temperatures.

Wind Profiler RASS (Bragg RASS)

Adding a sound source to a radar wind profiler yields a Bragg RASS or wind-temperature radar (Fig. 23.7). The first attempts to use such combinations were confronted with the problem that a Stokes shift rather than a Doppler shift was observed [23.40]. *Peters et al.* [23.41] showed that instead of measuring the Doppler frequency, the desired information can be extracted from the Bragg resonance curve. The Bragg resonance is obtained by varying the acoustic frequency and monitoring the backscatter maximum. Whereas the Doppler shift of the backscattered electromagnetic radiation provides information on the speed of sound when using a Doppler RASS, the Bragg resonance provides the acoustic wavelength when using a Bragg RASS (i.e., the acoustic wavelength is measured instead of the speed of sound). To achieve this, a Bragg RASS continuously transmits an acoustic frequency spectrum which is centered on the Bragg resonance frequency. This is in marked contrast to the single pulses transmitted by a Doppler RASS.

23.4.3 Comparison of the Methods

Different types of sodars and RASS have been developed for different measurement purposes, although the presence of various types also reflects the historical development of these instruments. Table 23.7 gives a concise overview of the advantages and disadvantages

Table 23.7 Advantages and disadvantages of the different types of sodars and RASS

Device	Advantages	Disadvantages
Sodar with antennas	Higher vertical range	Heavier instrument—a lorry is needed for deployment
Phased-array sodar	Smaller and lighter instrument—can be transported by a sport utility vehicle (SUV)	Reduced vertical range
Minisodar ($f_a \gtrsim 4000$ Hz)	Higher vertical resolution	Limited vertical range (200–300 m)
Bistatic/multistatic sodar	Velocity fluctuations also produce backscatter when using a multistatic sodar, all three wind components can be measured in the same atmospheric volume	More complicated deployment—all receivers must be connected to the grid and to data transfer, still very experimental
Multifrequency sodar	Higher signal-to-noise ratio, higher range	Enhanced electronics, noise interference
Non-Doppler sodar	Simpler technique and data evaluation	No wind velocity can be obtained
Doppler RASS	Higher vertical resolution, relatively portable, simpler technology, less expensive	Lower range
Wind profiler RASS	Lower vertical resolution	Higher range, not usually portable, more complicated technology, expensive

Fig. 23.7 A Bragg RASS with the radar instrumentation (wind profiler radar) at the center and additional acoustic sources (orange cylinders) next to it. The whole system is surrounded by a fence to prevent interference from other manmade sources of electromagnetic waves (e.g., radar and television emitters) (photo © Stefan Emeis)

of the different types of sodars and RASS. The first six rows refer to sodars, and the last two rows to RASS. Note that the first four rows refer to instruments with different layouts. The advantages and disadvantages presented in rows 5 and 6 could—at least in principle—apply to any of the sodars referred to in rows 1–4.

23.5 Specifications

This section summarizes information on the measured parameter accuracies and ranges that can be obtained with sodar and RASS measurements. Noise protection rules and electromagnetic permit procedures are also discussed.

23.5.1 Measured Parameter Accuracies and Ranges

The measured parameter accuracies and ranges for sodars and RASS are summarized in Table 23.8. The range of wind speed values is limited by the accuracy at the lower end and by environmental noise and noise generated at the edges of the instrument at the upper end. The range of temperature values is only limited by the selected frequency range of the acoustic chirp (Doppler RASS) or the continuous acoustic signal (Bragg RASS).

23.5.2 Permits Required for RASS Operation

RASS devices emit radio waves that can interfere with other telecommunication services. National regulations on the allocation of operating frequencies must

Table 23.8 The accuracies and ranges of wind, turbulence, and temperature measurements obtained using sodars and RASS (based on [23.4, 9])

Parameter	Accuracy	Range
Wind speed (radial wind component)	$0.3\,\mathrm{m\,s^{-1}}$ for a single measurement; $0.05\,\mathrm{m\,s^{-1}}$ for the average of 40 measurements	0.05 to $\approx 20\,\mathrm{m\,s^{-1}}$
Wind speed (computed from the radial wind components)	$0.3–0.5\,\mathrm{m\,s^{-1}}$ for the average of 10 min of measurements	0.3 to $\approx 20\,\mathrm{m\,s^{-1}}$
Standard deviation of the vertical wind component	$0.16\,\mathrm{m\,s^{-1}}$ based on 40 measurements	0.16 to several $\mathrm{m\,s^{-1}}$ (no real upper limit)
Temperature	0.5 K; error of 1.7 K per $1\,\mathrm{m\,s^{-1}}$ of the unknown vertical wind component (averaging reduces this error; see (23.7))	No principal limit for the temperature range; it depends on the width of the frequency spectrum of the acoustic signal. Doppler RASS: no temperature data for wind speeds $\gtrsim 12–15\,\mathrm{m\,s^{-1}}$ because the wind drifts the sound pulse away from the focus of the receiving electromagnetic antenna

therefore be observed when using such systems. In Germany, the standard RegTP 321 ZV 044 [23.42], which references certain international regulations, applies in this context. An application for a permit to operate a RASS must be filed with the Bundesnetzagentur für Elektrizität, Gas, Telekommunikation, Post und Eisenbahnen (RegTP; the Federal Agency for Electricity, Gas, Telecommunication, Post and Railroad Grids).

23.5.3 Compliance with Noise Regulations

In Germany, the operator of a sodar or a RASS must comply with standards and statutory regulations that are relevant to noise, such as the EU's Noise Directive 2003/10/EC [23.43], the German Federal Immission Protection Law (BImSchG [23.44]), or the guideline VDI 2058 Part 2 [23.45]. An a priori application for a permit is not required in Germany.

23.6 Quality Control

General quality assurance and quality control procedures are described in Chap. 3. In this section we focus on quality assurance and quality control procedures that are specific to sodar and RASS devices.

The quality of wind and temperature data from sodar and RASS devices depends mainly on the signal-to-noise ratio (i.e., the intensity ratio of the backscattered signal to the background noise) and the quality of the data evaluation algorithm used. Sodar and RASS devices are usually shipped with built-in data evaluation algorithms. The manufacturers of these devices should indicate the minimum signal-to-noise ratio that must be attained in order to extract meaningful data from the built-in data evaluation algorithms. The temporal and vertical consistency of the final wind and temperature data provides valuable insight into the reliability of the retrieved data. Table 23.9 gives an overview of common instrument errors.

The signal-to-noise ratio usually decreases with increasing range because the backscattered sound intensity decreases with the square of the range (Sect. 23.3.1). The maximum range is frequency de-

Table 23.9 Typical measurement errors with sodars or RASS

Instrument	Error(s)	Reason(s)
Sodar	No wind data	Antenna is covered with snow, technical failure of instrument
Sodar	Low vertical range, spatially and temporally inconsistent data	Signal-to-noise ratio is too low due to ambient noise (could be caused by rain or very high wind speeds), intensity of atmospheric turbulence is too low to cause sufficient acoustic backscatter
Sodar	Low vertical range in wind data during morning or afternoon	Atmosphere nearly adiabatic
Sodar	Wind speed minima in vertical profiles always occur at the same height (and backscatter intensity is enhanced)	Fixed echo, azimuth angle of antenna must be adjusted or a better measurement site is needed
RASS	No temperature data	Technical failure of instrument
RASS	Missing temperature data for certain heights and for a limited period	Excessive wind speeds (often due to nocturnal low-level jets) have blown the signal away from the focus of the receiving electromagnetic antenna

pendent (Sect. 23.3.1). The signal-to-noise ratio can be strongly influenced by environmental noise at the measurement site. Noise with the same frequency as the emitted sound pulses is especially problematic. Measurement sites in noisy industrial areas or close to motorways or railway lines should be avoided. The signal-to-noise ratio is also degraded by strong winds, as such winds can generate noise in the vicinity of the instrument or even at the edges of the instrument itself.

Some manufacturers also supply data processing software with their instruments. Such software often include visualization tools (e.g., to display time–height cross-sections of the retrieved data), printing options, and data export options. Key parameters that can be entered into the software include temporal and vertical averaging intervals and the start and end dates of the data to be processed.

Some manufacturers provide access to the raw data obtained by the instruments. The analysis of such raw data requires special skills. The processing of raw data may be helpful when attempting to detect and explain inconsistencies in the data sets or to calculate nonstandard output variables.

23.6.1 Wind Speed Calibration

Wind speeds from sodar and RASS devices do not require calibration as long as signal-to-noise ratios are high enough to permit the accurate measurement of the Doppler-induced frequency shift using the built-in data evaluation algorithm. Wind speed data are obtained from Doppler shift analysis using a basic physical principle that does not require any calibration. Nevertheless, it is useful to check the resulting data against the corresponding data provided by a cup anemometer or a sonic anemometer on a mast. Note that it is important to take differences in measurement principles (volume measurements with a sodar or RASS and almost point measurements with a cup or sonic anemometer) into account when comparing data from remote-sensing instruments with in-situ data.

23.6.2 Temperature Calibration

Temperature data from a RASS device do not require calibration as they are derived using a basic physical phenomenon: the detection of the speed of sound in air. This speed is a function of temperature and humidity only (see Sect. 23.3.1). Nevertheless, it may be useful to check the data against that afforded by a thermometer. Again, differences in measurement principles (volume measurements with a RASS and almost point measurements with a cup anemometer) should be taken into account when comparing data from remote-sensing instruments with in-situ data.

23.6.3 Specific Quality Control Methods

The calculation of wind speeds using monostatic remote-sensing devices such as sodars and RASS is based on the assumption that the streamlines are straight (no curvature in any direction) within the measurement volume defined by the separate beams in the Doppler beam swinging technique (see Sect. 23.4.1) or by the walls of the cone in conical scanning. The presence of streamlines that are curved towards the instrument causes the wind speed to be underestimated, whereas the presence of streamlines that are bent away from the instrument leads to an overestimated wind speed [23.46]. Thus, wind data from ground-based remote sensing on a hilltop are lower than the true wind speeds above the instrument, whereas wind data obtained in a valley are higher than the true wind speeds. Some manufacturers claim that they have built-in corrections for streamline curvature in their evaluation algorithms. These corrections cannot be rated here, because the manufacturers do not disclose how their algorithms calculate such corrections. The best way to determine the necessary corrections to the measurements is to run a flow model in conjunction with the instrument. This curvature problem occurs with sodars as well as with wind lidars (Chap. 27).

Measured wind speeds and turbulence data (i.e., the variance of the vertical wind component) must be checked for the impact of fixed echoes (Sect. 23.3.1). Fixed echoes lead to wind speeds that are lower than they should be because reflections from immobile objects are included in the data. Fixed echoes usually occur at a certain height above the ground that corresponds to the direct (diagonal) distance between the remote-sensing device and the object that is generating the fixed echoes. Thus, wind speeds that are consistently lower than expected at a particular height may be indicative of fixed echoes. Another clue that fixed echoes are occurring is the presence of very high backscatter intensities, because most solid objects reflect sound waves much better than the atmosphere does. It is not possible to correct for fixed echoes a posteriori. The best way to deal with them is to discard the flawed wind and turbulence data.

Temperature data are not influenced by curved streamlines because temperature is derived using vertical sound emission only. Temperature sounding also does not suffer from fixed echoes. Thus, for a Doppler

Table 23.10 Maintenance of sodars and RASS

Maximum interval	Sodar (all types)	Doppler RASS	Bragg RASS
Daily	Check incoming data for consistency		
Daily	Perform a visual check of the instrument (unless the site is within a well-guarded and supervised area)		
Every 3 months	Check that all loudspeakers are functioning properly	Check that all loudspeakers and antennas are functioning properly	
Every 2 years	Check all electrical cables and devices		

RASS, the maximum range of the temperature data is usually considerably higher than the maximum range of the wind data.

Temperature determination can be hampered by high wind speeds. In this case, the sound waves emitted from the Doppler RASS are blown outside the focus of the receiving radio antenna. Thus, it is sometimes impossible to detect the temperature in areas with high wind speeds caused by nocturnal low-level jets. Depending on the size of the instrument, temperature determination can be problematic when wind speeds are $> 10{-}15\,\mathrm{m\,s^{-1}}$.

23.7 Maintenance

Just like any device that is connected to the electrical grid and operated outdoors, sodars and RASS devices require technical and electrical maintenance. No additional substances such as gases or liquids have to be supplied during the measurements. The overall amount of maintenance required for such instruments is low (see Table 23.10). Manufacturers' instructions should be followed, and software updates should be uploaded as soon as possible.

A direct connection to the instrument's computer via the internet or mobile telecommunications services is advisable. Error messages issued by the software can give hints about malfunctions. Daily data transfer from the instrument to the operator's institution is recommended. Regular checks of the consistency of the incoming data can provide further insight into potential malfunctions.

23.8 Applications

The most informative data products obtained from ground-based remote-sensing instruments such as sodars and RASS devices are time–height cross-sections of wind speed, wind direction, the vertical component of turbulence, and temperature. The vertical profiles of these parameters can be extracted from time–height cross-sections. Time series of selected parameters (e.g., mixed-layer height) can also be extracted.

An example of real-world data obtained using a sodar is presented in Fig. 23.8, which shows the daily variation in the horizontal wind in an alpine valley during a clear-sky day. Steady southerly to southwesterly winds representing the down-valley flow are seen to occur from 10 p.m. to 8 a.m. (GMT+1), whereas turbulent northerly to northeasterly winds representing the up-valley flow are observed between 10 a.m. and 8 p.m.

Another real-world dataset provided by a sodar is depicted in Fig. 23.9, which shows a perfect example of the measurement of wind speeds in a nocturnal low-level jet. The maximum wind speed along the axis of the jet is $\approx 12\,\mathrm{m\,s^{-1}}$, whereas the wind speed underneath and above the jet is $\approx 5\,\mathrm{m\,s^{-1}}$. The measurements were performed in a very quiet environment, which made it possible to observe the upper part of the low-level jet, where the wind speed decreases with height (very often, a sodar can only measure wind speeds below the jet axis, not those above it).

A final example (Fig. 23.10) shows the diurnal temperature variation in the lower atmospheric boundary layer on a clear-sky day, as measured with a Doppler RASS. Potential temperature data are presented. In the early morning (between 2 a.m. and 10 a.m. GMT+1), cold air (blue) occurs near the surface. Warmer air (green) occurs above the cold air. At ≈ 10 a.m., vertical mixing starts, and soon afterwards the air is well mixed vertically until ≈ 6 p.m. Then cooling sets in again near the surface while the air remains warm above. The white area in the upper right corner corresponds to missing data. Data are missing from this region because high wind speeds caused by a low-level jet drifted the sound pulse from the Doppler RASS out of the focus of the receiving electromagnetic antenna.

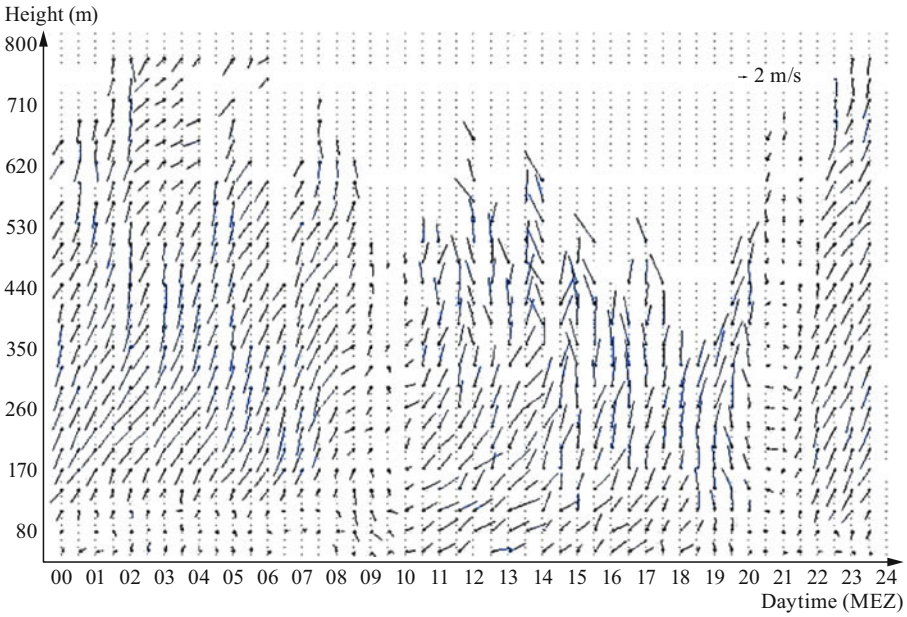

Fig. 23.8 Time–height cross-section of horizontal wind vectors measured over the course of one day (*x*-axis) for heights of 50—800 m AGL using a three-antenna sodar. Time resolution: 30 min; height resolution: 30 m. Arrow length is proportional to wind speed (see the legend in the *upper right corner*). Arrow direction indicates the wind direction (upward: wind from the south; to the right: wind from the west; etc.). Measurements were performed in an almost north–south-oriented valley on the northern side of the Alps at Oberau (Germany) on 8 May 1998

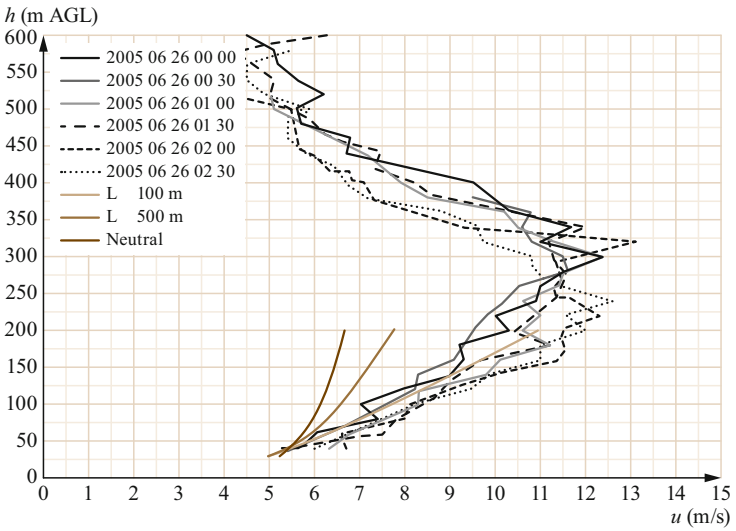

Fig. 23.9 Nocturnal vertical wind-speed profiles obtained with a three-antenna sodar; the profiles show the presence of a low-level jet at $\approx$ 300 m *AGL*. Six wind speed profiles (each averaged over 30 min) obtained for heights ranging from 40 to 600 m AGL (vertical resolution: 20 m) are plotted. The measurements were performed at the Charles-de-Gaulle Airport in Paris (France) during the first three hours of 26 June 2005

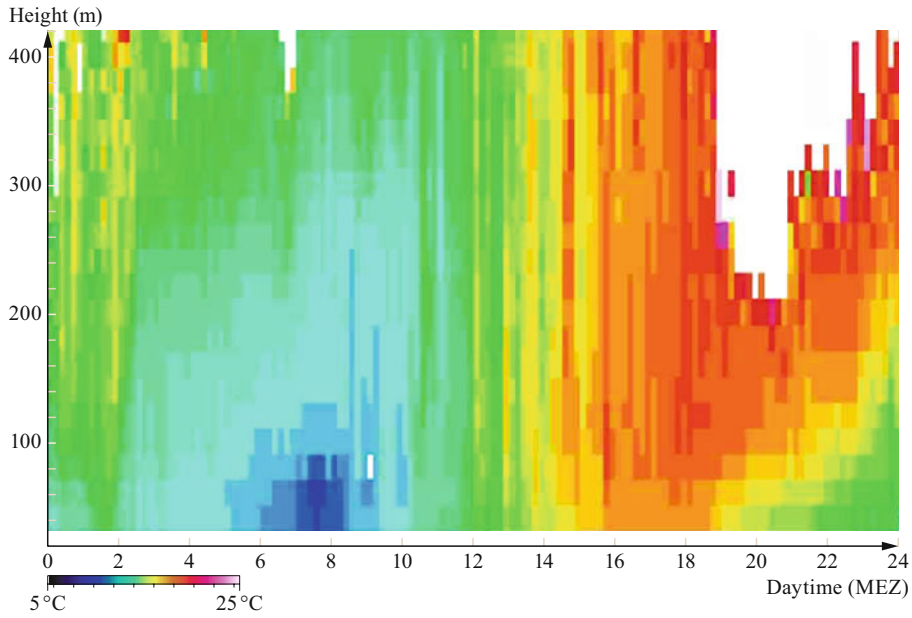

Fig. 23.10 Time–height cross-section of potential temperatures on a clear-sky day measured over a period of 24 h (local time) for heights of 40–420 m (vertical resolution: 20 m) using a Doppler RASS. *Colors* (see the color bar at the *lower right*) indicate potential temperatures ranging from 5 °C (*dark blue*) to 25 °C (*purple*). The measurements were performed at the northern outskirts of Augsburg (Germany) on 6 April 2009

23.9 Future Developments

Although they are relatively old techniques, there is still a need for these vertical sounding devices that actively emit sound waves. While wind profile measurements are increasingly being performed with wind lidars rather than sodars (because wind lidars offer enhanced data availability and do not suffer from environmental interference), RASS are still the best available devices for measuring the temperature profiles of the lower regions of the atmospheric boundary layer. Passive radiometers have much poorer vertical resolution, meaning that they are generally not well suited to boundary layer studies. Raman lidars also have deficiencies, especially during the daytime, when the intense short-wave solar radiation causes interference.

Apart from classical scientific boundary layer studies, new fields of application for ground-based remote sensing have developed in recent decades, which has reinvigorated the development of acoustic sounders. One of the most important of these new fields of application is wind energy (see Chap. 51 and [23.3]). Wind energy requires highly vertically and temporally resolved wind, turbulence, and temperature profile data for site assessments, yield forecasts, and load assessments. While site and load assessments are especially valuable for the manufacturers of wind turbines, yield forecasts are mandatory for electrical grid operators and for successful trade actions at energy exchanges.

Another field in which sodars and RASS have been deployed in the last few decades is urban studies. However, in this case, the active emission of sound waves is a disadvantage of these instruments, as it is becoming increasingly difficult to find acceptable measurement sites for sodars and RASS in densely populated areas. Therefore, researchers are attempting to develop measurement configurations that shield urban populations from the emitted sound waves. One such configuration is the bistatic sodar (see Sect. 23.4.1), in which the vertical emission of sound pulses is well shielded and the receiver is located away from the instrument.

Methods of correcting wind profile data from sodars (and wind lidars) located in complex terrain (see Sect. 23.6.3) are still being developed. Some manufacturers offer built-in correction algorithms, although they do not explain how they work. Others suggest running

simple flow models in parallel with the measurements to obtain the necessary corrections. Attempts to produce feasible correction algorithms for ground-based monostatic wind profilers operating in complex terrain will continue even if sodars start to disappear, because wind lidars have the same problem.

In the long run, the importance of acoustic sounding techniques will decrease.

23.10 Further Reading

A general overview of acoustics can be found in

> Rossing, T.D. (ed.): Springer Handbook of Acoustics, 2nd edn. (Springer, 2014).

The standard resource on sodars is the book by *Bradley* [23.6]. There is no corresponding book on RASS devices. The bilingual VDI Guideline 3786 Part 18 [23.9] is most probably among the most concise sources of information in this regard.

A general overview of ground-based remote sensing of the atmospheric boundary layer can be found in [23.1].

A short overview of all atmospheric measurement techniques can be found in

> Emeis, S.: Measurement Methods in Atmospheric Sciences. In-situ and remote. (Borntraeger, Stuttgart 2010), XIV + 257 pp.

The 2014 edition of the WMO Guide to Meteorological Instruments and Methods of Observations (WMO No. 8) covers radar in detail but mentions sodars and RASS only briefly (in Chapter 5 of Part II).

References

23.1 S. Emeis: Surface-Based Remote Sensing of the Atmospheric Boundary Layer. In: *Atmospheric and Oceanographic Sciences Library*, Vol. 40 (Springer, Berlin, Heidelberg 2011)

23.2 S. Emeis: Upper limit for wind shear in stably stratified conditions expressed in terms of a bulk Richardson number, Meteorol. Z. **26**, 421–430 (2017)

23.3 S. Emeis: *Wind Energy Meteorology – Atmospheric Physics for Wind Power Generation*, Green Energy and Technology, 2nd edn. (Springer, Berlin, Heidelberg 2018)

23.4 VDI 3786 Part 11:2015-07: *Environmental Meteorology: Ground-Based Remote Sensing of the Wind Vector and the Vertical Structure of the Boundary Layer – Doppler Sodar* (Beuth, Berlin 2015)

23.5 G. Peters: SODAR – Ein akustisches Fernmeßverfahren für die untere Atmosphäre, Promet **21**, 55–62 (1991)

23.6 S. Bradley: *Atmospheric Acoustic Remote Sensing – Principles and Applications* (CRC Press, Boca Raton 2007)

23.7 W.H. Bragg, W.L. Bragg: The reflection of X-rays by crystals, Proc. R. Soc. A **88**, 428–438 (1913)

23.8 J.M. Marshall, A.M. Peterson, A. Barnes: Combined radar-acoustic sounding system, Appl. Opt. **11**, 108–112 (1972)

23.9 VDI 3786 Part 18: *Environmental Meteorology: Ground-Based Remote Sensing of Temperature Radio-Acoustic Sounding Systems (RASS)* (Beuth, Berlin 2010)

23.10 D.A.M. Engelbart, J. Bange: Determination of boundary-layer parameters using wind profiler/RASS and sodar/RASS in the frame of the LITFASS project, Theor. Appl. Climatol. **73**, 53–65 (2002)

23.11 VDI 3786 Part 17: *Environmental Meteorology – Ground-Based Remote Sensing of the Wind Vector – Wind Profiler Radar* (Beuth, Berlin 2007)

23.12 ISO 9613-1:1993-06: *Acoustics; Attenuation of Sound During Propagation Outdoors; Part 1: Calculation of the Absorption of Sound by the Atmosphere* (International Organization for Standardization, Geneva 1993)

23.13 R. Wexler, D.M. Swingle: Radar storm detection, Bull. Am. Meteorol. Soc. **28**, 159–167 (1947)

23.14 G.W. Gilman, H.B. Coxhead, F.H. Willis: Reflection of sound signals in the troposphere, J. Acoust. Soc. Am. **18**, 274–283 (1946)

23.15 V.I. Tatarskii: *The Effect of the Turbulent Atmosphere on Wave Propagation* (Kefer Press, Jerusalem 1971)

23.16 M.A. Kallistratova: An experimental investigation in the scattering of sound in the turbulent atmosphere, Dokl. Akad. Nauk. SSSR **125**, 69–72 (1959)

23.17 M.A. Kallistratova, I.V. Petenko, R.D. Kouznetsov, S.N. Kulichkov, O.G. Chkhetiani, I.P. Chunchusov, V.S. Lyulyukin, D.V. Zaitseva, N.V. Vazaeva, D.D. Kuznetsov, V.G. Perepelkin, G.A. Bush: Sodar sounding of the atmospheric boundary layer: Review of studies at the Obukhov Institute of Atmospheric Physics, Russian Academy of Sciences, Izv. Atmos. Ocean. Phys. **54**, 242–256 (2018)

23.18 L.G. McAllister, J.R. Pollard, A.R. Mahoney, P.J.R. Shaw: Acoustic sounding – A new approach to the study of atmospheric structure, Proc. IEEE **57**, 579–587 (1969)

23.19 ECMA-108:2010-12: *Measurement of High-Frequency Noise Emitted by Information Technology and Telecommunications Equipment* (European Computer Manufacturers Association, Geneva 2010)
23.20 K. Attenborough: Sound propagation in the atmosphere. In: *Handbook of Acoustics*, 2nd edn., ed. by T.D. Rossing (Springer, New York 2014) pp. 117–155
23.21 O. Reitebuch: *SODAR-Signalverarbeitung von Einzelpulsen zur Bestimmung hochaufgelöster Windprofile*, Schriftenreihe des Fraunhofer-Instituts Atmosphärische Umweltforschung, Vol. 62 (Shaker, Aachen 1999)
23.22 F. Beyrich: Mixing height estimation from sodar data – A critical discussion, Atmos. Environ. **31**, 3941–3953 (1997)
23.23 D.N. Asimakopoulos, C.G. Helmis, J. Michopoulos: Evaluation of SODAR methods for the determination of the atmospheric boundary layer mixing height, Meteorol. Atmos. Phys. **85**, 85–92 (2004)
23.24 S. Emeis, M. Türk: Frequency distributions of the mixing height over an urban area from SODAR data, Meteorol. Z. **13**, 361–367 (2004)
23.25 S. Emeis, C. Jahn, C. Münkel, C. Münsterer, K. Schäfer: Multiple atmospheric layering and mixing-layer height in the Inn valley observed by remote sensing, Meteorol. Z. **16**, 415–424 (2007)
23.26 S. Emeis, K. Schäfer, C. Münkel: Surface-based remote sensing of the mixing-layer height – A review, Meteorol. Z. **17**, 621–630 (2008)
23.27 J. Röttger, J. Klostermeyer, P. Czechowsky, R. Rüster, G. Schmidt: Remote sensing of the atmosphere by VHF radar experiments, Naturwissenschaften **65**, 285–296 (1978)
23.28 R.L. Coulter, T.J. Martin: Results from a high-power, high-frequency sodar, Atmos. Res. **20**, 257–269 (1986)
23.29 Y. Ito, Y. Kobori, M. Horiguchi, M. Takehisa, Y. Mitsuta: Development of wind profiling sodar, J. Atmos. Ocean. Technol. **6**, 779–784 (1989)
23.30 D.W. Thomson, R.L. Coulter: Analysis and simulation of phase coherent acdar sounding measurements, J. Geophys. Res. **79**, 5541–5549 (1974)
23.31 M.L. Wesely: The combined effect of temperature and humidity fluctuations on refractive index, J. Appl. Meteorol. **15**, 43–49 (1976)
23.32 R.L. Coulter, K.H. Underwood: Some turbulence and diffusion parameter estimates within cooling tower plumes derived from sodar data, J. Appl. Meteorol. **19**, 1395–1404 (1980)
23.33 K.H. Underwood: *Sodar Signal Processing Methods and the Risø-78 Experiment*, PhD thesis (Pennsylvania State Univ., University Park 1981)
23.34 S. Bradley, S. von Hünerbein, T. Mikkelsen: A bistatic sodar for precision wind profiling in complex terrain, J. Atmos. Ocean. Technol. **29**, 1052–1061 (2012)
23.35 S. Bradley, J. Barlow, J. Lalley, C. Halios: A sodar for profiling in a spatially inhomogeneous urban environment, Meteorol. Z. **24**, 615–624 (2015)
23.36 A. Strehz, S. Bradley: Mast comparisons for a new bistatic SODAR design. In: *17th Int. Symp. Adv. Bound.-Layer Remote Sens. (ISARS) Auckland* (2014)
23.37 R. Kouznetsov: The multi-frequency sodar with high temporal resolution, Meteorol. Z. **18**, 169–173 (2009)
23.38 S.G. Bradley: Use of coded waveforms for SODAR systems, Meteorol. Atmos. Phys. **71**, 15–23 (1999)
23.39 C.S. Bonner, M.C.B. Ashley, J.S. Lawrence, J.W.V. Storey, D.M. Luong-Van, S.G. Bradley: Snodar: A new instrument to measure the height of the boundary layer on the Antarctic plateau, Proc. SPIE **7014**, 70146I (2008)
23.40 A.I. Kon, V.I. Tatarskii: The scattered signal frequency spectrum for radio acoustical atmospheric soundings, Izv. Atmos. Ocean. Phys. **16**, 142–148 (1980)
23.41 G. Peters, H. Timmermann, H. Hinzpeter: Temperature sounding in the planetary boundary layer by RASS-system analysis and results, Int. J. Remote Sens. **4**, 49–63 (1983)
23.42 RegTP: Zulassungsvorschrift für Windprofil-Messradaranlagen, RegTP 321 ZV 044, Juli 1999. In: Amtsblatt der Regulierungsbehörde für Telekommunikation und Post, Nr. 1 vom 12.01.2000
23.43 Directive 2003/10/EC of the European Parliament and of the Council of 6 February 2003 on the Minimum Health and Safety Requirements Regarding the Exposure of Workers to the Risks Arising from Physical Agents (Noise). https://eur-lex.europa.eu/legal-content/EN/TXT/?uri=CELEX:02003L0010-20081211, current version (2019), Accessed 08. July 2021
23.44 Bundes-Immissionsschutzgesetz: Gesetz zum Schutz vor schädlichen Umwelteinwirkungen durch Luftverunreinigungen, Geräusche, Erschütterungen und ähnliche Vorgänge (BImSchG). (in German http://www.rechtliches.de/info_BImSchG.html) (2017), Accessed 08. July 2021
23.45 VDI 2058 Part 2: *Assessment of Noise with Regard to the Risk of Hearing Damages (Draft)* (Beuth, Berlin 2017)
23.46 S. Bradley, A. Strehz, S. Emeis: Remote sensing winds in complex terrain – A review, Meteorol. Z. **24**, 547–555 (2015)

Stefan Emeis

Institute of Meteorology and Climate Research
Karlsruhe Institute of Technology (KIT)
Garmisch-Partenkirchen, Germany
stefan.emeis@kit.edu

Stefan Emeis is an unsalaried Professor of Meteorology at the University of Cologne, group leader at KIT, and editor-in-chief of *Meteorologische Zeitschrift*. His research mainly involves ground-based remote sensing of the atmospheric boundary layer. He has written books on measurement techniques and wind energy, organized conferences (e.g., ISARS 13, METTOOLS VI), and was awarded the Honorary Medal of the VDI and the Reinhard Süring Medal from the German Meteorological Society.